On the Uniqueness of Clifford Torus with Prescribed Isoperimetric Ratio

Thomas Yu* Jingmin Chen†

March 26, 2020

Abstract:
The Marques-Neves theorem asserts that among all the torodial (i.e. genus 1) closed surfaces, the Clifford torus has the minimal Willmore energy $\int H^2\,dA$. Since the Willmore energy is invariant Möbius transformations, it can be shown that there is a one-parameter family, up to homotheties, of genus 1 Willmore minimizers. It is then a natural conjecture that such a minimizer is unique if one prescribes its isoperimetric ratio. In this article, we show that this conjecture can be reduced to the positivity question of a polynomial recurrence.

Acknowledgments. This work is partially supported by NSF grants DMS 0915068 and DMS 1115915. We thank Robert Kusner for bringing to our attention the uniqueness problem. Also, we are grateful to Manuel Kauers, Stephen Melczer and Pierre Lairez for sharing their expertise in P-recurrences.

Keywords: Canham-Evans-Helfrich model, Willmore energy, Clifford torus, Möbius geometry, Marques-Neves theorem, Uniqueness, P-recurrence, Special functions, Positivity

1 Uniqueness problem in the Canham-Evans-Helfrich model

Why do all humans of all races occur to have the same biconcave shaped red blood cells? This apparent uniqueness might have intrigued biologists since the invention of microscope. The seminal work of Canham [4], Helfrich [10] and Evans [8] suggests that bending elasticity, induced by curvature, plays the key role in driving the geometric configurations of such membranes.

The so-called spontaneous curvature model of Helfrich suggests that a biomembrane surface S configures itself to minimize $\int_S H^2 dA$ subject to the area, volume and area difference (related to the bilayer characteristics) constraints, i.e. S solves the variational **Helfrich problem**

$$\min_S W(S) := \int_S H^2\,dA \text{ s.t. } \begin{cases} \text{(i)} & A(S) := \int_S 1\,dA = A_0, \\ \text{(ii)} & V(S) := \frac{1}{3}\int_S [x\hat{\mathbf{i}} + y\hat{\mathbf{j}} + z\hat{\mathbf{k}}]\cdot\hat{\mathbf{n}}\,dA = V_0, \\ \text{(iii)} & M(S) := -\int_S H\,dA = M_0. \end{cases} \tag{1.1}$$

Here $H = (\kappa_1 + \kappa_2)/2$ is the mean curvature. (We assume that the normal of any closed orientable surface points outward. In particular, it means $H < 0$ for a sphere.) In (ii), $V(S)$ is the enclosed volume. The connection of (iii) to bilayer area difference comes from the relation $-\int_S H dA = \lim_{\varepsilon\to 0}\frac{1}{4\varepsilon}(\text{area}(S_{+\varepsilon}) - \text{area}(S_{-\varepsilon}))$, where $S_{+\varepsilon}$ and $S_{-\varepsilon}$ are the 'ε-offset surfaces', and that the thickness of the lipid bilayer, 2ε, is negligible compared to the size of the vesicle. The constraint values A_0, V_0 and M_0 are determined by physical conditions (e.g. temperature, concentration). $W(S)$ is called the **Willmore energy** of the surface

*Department of Mathematics, Drexel University. Email: yut@drexel.edu. He is supported in part by the National Science Foundation grants DMS 0512673 and DMS 0915068.

†Citigroup Global Markets Inc., 390 Greenwich Street, New York, NY 10013, U.S.A.. Email: jingmchen@gmail.com.

S. When the area-difference constraint (iii) is omitted, the variational problem is referred to as the **Canham problem**. When even the volume constraint (ii) is omitted, the variational problem is referred to as the **Willmore problem**. In this case, there is essential no constraint as W is scale-invariant. In any case, the area constraint (i) only fixes the scale; see the discussion around (1.3) below.

It is observed experimentally that no topological change occurs in any accessible time-scale, so the Helfrich, Canham or Willmore problems ask for a minimizer S over all orientable closed surface with a fixed genus g. Spherical ($g = 0$) vesicles are the most common among naturally occurring biomembranes, although higher genus ones have been synthesized in the laboratory [21, 13, 24]. The Canham, Helfrich and related models explain the large variety of shapes observed in even a closed vesicle with a spherical topology.

At a mathematical level, the existence of solution for the Canham problem is studied in [23] for the genus 0 case and in [17] for arbitrary genus. Uniqueness, however, seems to be never addressed mathematically.

It is well-known from [2, 6] that the quantity $(H^2 - K)dA$ is invariant under Möbius transformations, i.e. any transformation from the group of translations (3 dimensions), rotations (3 dimensions), uniform scalings (1 dimension) and ***sphere inversions*** (3 dimensions). If we denote this group by Möb(3); we have $\dim(\text{Möb}(3)) = 3+3+1+3 = 10$. Here, by sphere inversion, we mean inversion about a unit sphere centered at any point in 3-space, i.e.

$$i_{\mathbf{a}}(\mathbf{x}) = t_{\mathbf{a}} \circ i \circ t_{-\mathbf{a}}, \quad \text{where} \quad i(\mathbf{x}) := \frac{\mathbf{x}}{\|\mathbf{x}\|^2}, \quad t_{\mathbf{a}}(\mathbf{x}) = \mathbf{x} + \mathbf{a}. \tag{1.2}$$

(Sphere inversion w.r.t. a sphere with a non-unit radius can be written as one of the form (1.2) composed with a scaling.)

The constraint functionals, namely A, V and M are only invariant under the smaller group of rigid motions SE(3). Due to the scale-invariance of the Willmore energy, the solution, up to homothety, of any of the Willmore, Canham or Helfrich problems depends only on the *reduced volume* and *reduced total mean curvature* defined by:

$$v_0 := V_0/[(4\pi/3)(A_0/4\pi)^{3/2}], \quad m_0 := M_0/[4\pi(A_0/4\pi)^{1/2}]. \tag{1.3}$$

This terminology is used by a group of biophysicists who have done a plethora of computational and physical experiments exploring the shapes of phospholipid vesicles. Note that v_0 is essentially what a geometer would call the *isoperimetric ratio*. By the isoperimetric inequality, we have $v_0 \in (0, 1]$ and $v_0 = 1$ is uniquely realized by a round sphere.

From now on, we think of two surfaces as the same, or that they have the same (Euclidean) shape, when they are homothetic. By uniqueness of solution (of any one of the Helfrich, Canham or Willmore problems) we mean there is only one solution surface up to homothety.

1.1 Non-uniqueness in $g \geqslant 2$

Given any minimizer of a Canham or Helfrich problem, one may apply to it the three dimensional family of sphere inversions (1.2) and expect to have enough degrees of freedom to satisfy the reduced volume constraint or reduced volume plus mean curvature constraints, yielding a two- or one-parameter (respectively) family of non-homothetic solutions. This suggests that one should not expect uniqueness in general.

This hasty dimension count is easily seen to be flawed in at least specific cases. For instance,

- When $g = 0$, the unconstrained Willmore minimizer is the round sphere and is unique, which is clearly **invariant under the whole Möbius group**.
- When $g = 1$, the unconstrained Willmore minimizers are exactly the stereographic images into $\mathbb{R}^3$ of the Clifford torus $\{[\cos u, \sin u, \cos v, \sin v]^T/\sqrt{2} : u, v \in [0, 2\pi]\}$ in $\mathbb{S}^3$. For any such Clifford torus in $\mathbb{R}^3$, its Euclidean shape is **invariant under 2 out of the three degrees of freedom of the sphere inversions in** (1.2). (In Section 2, we shall establish a precise version of this fact.)

So in the first case, if we choose v_0 and m_0 to be the reduced volume and total mean curvature of the round sphere, then the corresponding Canham or Helfrich problem must also have the round sphere as the unique solution. In the second case, if we choose v_0 and m_0 to be the reduced volume and total mean curvature of any Clifford torus, then we expect the corresponding Canham problem, and hence also the Helfrich problem, to have a unique solution. The latter observation will be the focus of this article.

The dimension count, however, sounds more convincing when the genus g is 2 or above. By Hurwitz's automorphisms theorem, there can only be a finite number – no more than $84(g-1)$ – conformal mappings leaving any compact genus g surface invariant under homothety. Since sphere inversions are conformal mappings, the three-dimensional family of sphere inversions (1.2), when applied to any fixed compact surface of genus $g \geqslant 2$, must generate a 3-dimensional family of non-homothetic surfaces.

However, uniqueness may still hold when $g \geqslant 2$. To understand it better, let us first observe that instead of the 3-dimensional family of sphere inversions (1.2), we can instead use the 3-dimensional family of special conformal transformations

$$\mathrm{SCT}_{\mathbf{a}} = i \circ t_{\mathbf{a}} \circ i, \quad \mathbf{a} \in \mathbb{R}^3. \tag{1.4}$$

This is because for every sphere inversion $i_{\mathbf{a}}$, there is a (orientation-reversing) homothety H such that $i_{\mathbf{a}} = H \circ \mathrm{SCT}_{i(\mathbf{a})}$. Moreover, since every transformation in Möb(3) is either a homothety, an inversion, or an homothety composed with an inversion[1], the non-homothetic copies of any surface S under Möb(3) can be found in $\{\mathrm{SCT}_{\mathbf{a}}(S) : \mathbf{a} \in \mathbb{R}^3\}$.

So part of the (non-)uniqueness analysis boils down to the understanding of the map

$$\mathbb{R}^3 \ni \mathbf{a} \overset{\Gamma_S}{\to} \begin{bmatrix} v(\mathrm{SCT}_{\mathbf{a}}(S)) \\ m(\mathrm{SCT}_{\mathbf{a}}(S)) \end{bmatrix} \in \mathbb{R}^2.$$

Here $v()$ and $m()$ are the reduced volume and reduced total mean curvature of the argument surface; and we call the map Γ_S. Being a nonlinear map, the mere fact that the co-domain has a lower dimension than the domain does *not* guarantee that the pre-image of a given point $[v_0, m_0]^T \in \mathrm{Image}(\Gamma_S)$ is non-unique. (E.g., for the map $(x_1, x_2, x_3) \mapsto x_1^2 + x_2^2 + x_3^2$, the pre-image of 0 is a singleton.) The implicit function theorem guarantees that if the differential of Γ_S at the origin is full rank, then indeed there is a curve through the origin, call it $\mathbf{a}(t)$, such that $\Gamma_S(\mathbf{a}(t)) = \Gamma_S(0)$. To conclude, if S is a particular solution of a genus $g \geqslant 2$ Helfrich problem, and if $\mathrm{rank}(d\Gamma_S|_0) = 2$, then there must be a one-parameter of non-homothetic solutions.

The use of special conformal transformation gives a nice expression for $d\Gamma_S|_0$:

$$\nabla v|_0 = 6v(0)(\mathbf{R}^A - \mathbf{R}^V), \quad \nabla m|_0 = 2m(0)(\mathbf{R}^A - \mathbf{R}^M),$$

where $\mathbf{R}^A$, $\mathbf{R}^V$ and $\mathbf{R}^M$ are the area, volume and mean curvature centers of S; see [24, Section 5.3.1]. Therefore $\mathrm{rank}(d\Gamma_S|_0) = 2$ exactly when the three centers are not collinear. Note that the latter condition says that S must have a certain degree of asymmetry. For instance, it rules out the case when S possesses 2 planes of mirror symmetry.

It is conjectured that the stereographic images of Lawson's minimal surface $\xi_{g,1}$ in $\mathbb{S}^3$ [19] are the only W-minimizer of genus g in $\mathbb{R}^3$. The stereographic images of $\xi_{2,1}$ attain many different values of reduced volume v_0 and reduced total mean curvature m_0. For many such values, it is observed in [13] that the corresponding centers are not collinear and hence there is a one-parameter family of solution surfaces. (However, it is not clear if a rigorous proof is available for this claim.) This non-uniqueness is called "conformal diffusion" in the biophysics literature and is observed experimentally in a laboratory setting [21].

1.2 Empirical Uniqueness in genus $g = 0$ and 1

For the genus 0 Canham problem, of which existence is shown for all $v_0 \in (0, 1]$ [23], it is observed from a lot of computations (e.g. [24, 7]) that the solution is unique and is a surface of revolution. When the

[1] This is a consequence of the proof of Liouville's theorem on conformal mappings; see, for example, [1, Page 92].

reduced volume v_0 is greater than a certain value approximately equal to 0.591, the solution surface appears to be have an additional plane of mirror symmetry orthogonal to the axis of revolution; in this case we expect $\mathbf{R}^A = \mathbf{R}^V$. When v_0 is smaller than 0.591, a phase transition occurs; the solution surface is a so-called stomatocyte, which still appears to be a surface of revolution but loses the additional plane of mirror symmetry. When $v_0 = 1$, the solution is a round sphere, when $v_0 \to 0$, the solution approaches a 'double sphere'.

For the genus 1 Canham problem, the existence is only established for v_0 in an (unknown) open interval containing

$$\big[(3/2)(2\pi^2)^{-1/4}, 1\big); \tag{1.5}$$

see [17]. This interval is also the set of reduced volume values attained by the Möbius transformations of the Clifford torus – see Figure 1 and the next section. The value $v_0 = (3/2)(2\pi^2)^{-1/4}$ is the reduced volume of the surface of revolution Clifford torus

$$T_{\sqrt{2}} = \Big\{ \big[\big(\sqrt{2} + \cos(v)\big)\cos(u),\ \big(\sqrt{2} + \cos(v)\big)\sin(u),\ \sin(v) \big] : u, v \in [0, 2\pi] \Big\}.$$

The uniqueness of the genus 1 Canham problem on the interval (1.5) is the focus of this paper. When $v_0 \in (0, (3/2)(2\pi^2)^{-1/4}]$, many computations suggest that the solution surface is unique and, similar to the genus 0 case, is a surface of revolution; see [24, 7] and the references therein.

We therefore have the following grand conjecture:

Conjecture 1.1. *The genus $g = 0$ or 1 Canham problem with any isoperimetric ratio constraint $v_0 \in (0, 1)$ has a unique solution up to homothety. Moreover,*

(i) when $g = 0$, for each $v_0 \in (0, 1]$ the unique solution is a surface of revolution;

(ii) when $g = 1$, for each $v_0 \in \big(0, (3/2)(2\pi^2)^{-1/4}\big]$, the unique solution is a surface of revolution;

(iii) when $g = 1$, for each $v_0 \in \big[(3/2)(2\pi^2)^{-1/4}, 1\big)$, the unique solution is a stereographic image into $\mathbb{R}^3$ of the Clifford torus $\{[\cos u, \sin u, \cos v, \sin v]^T/\sqrt{2} : u, v \in [0, 2\pi]\}$ in $\mathbb{S}^3$ or, equivalently, a Möbius transformation of $T_{\sqrt{2}}$.

(When $v_0 = 1$ and $g = 0$, it is clear that the solution is unique and is the round sphere. When $v_0 = 1$ and any $g \geqslant 1$, solution does not exist by the isoperimetric inequality.)

An obvious difficulty in proving the uniqueness conjecture in case (i) and (ii), or uniqueness/non-uniqueness in the higher genus cases, is that in general we do not have much information about the solutions of the Canham or Helfrich problems. As a starting point, we explore the third case of Conjecture 1.1, which appears to be the most tractable.

1.3 This paper

To establish Conjecture 1.1(iii), we propose the following four steps:

I. Prove that the set of all non-homothetic images of $T_{\sqrt{2}}$ under Möb(3) corresponds exactly to the one-parameter family

$$\{i_{(a,0,0)}(T_{\sqrt{2}}) : a \in [0, \sqrt{2} - 1)\}. \tag{1.6}$$

In other words, the cyclides depicted in Figure 1 are exactly the set of all non-homothetic Clifford tori. This is established in Theorem 2.4 of Section 2.

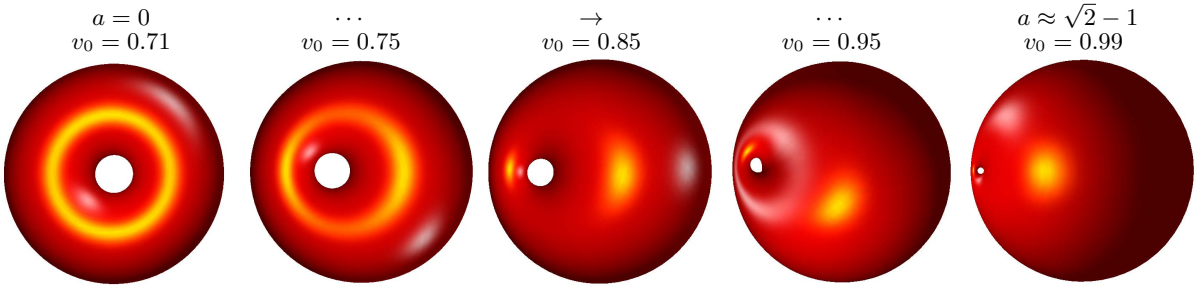

Figure 1: $i_{(a,0,0)}(T_{\sqrt{2}})$ as a increases from 0 to $\sqrt{2}-1$. By Theorem 2.4, these are all the possible non-homothetic images of $T_{\sqrt{2}}$ under Möb(3). By Pappus's centroid theorems, the reduced volume of the surface of revolution Clifford torus $T_{\sqrt{2}}$ is $(3/2)(2\pi^2)^{-1/4} \approx 0.71$. Notice that $i_{(0,0,0)}(T_{\sqrt{2}}) = T_{\sqrt{2}}$, viewing $T_{\sqrt{2}}$ as a point set. (As an oriented surface, $T_{\sqrt{2}}$ is turned inside out by $i = i_{(0,0,0)}$.) When a approaches $\sqrt{2}-1$, $i_{(a,0,0)}(T_{\sqrt{2}})$ approaches a round sphere, and hence should have a reduced volume close to 1; see Section 3 for a proof.

II. With this result, the conjecture follows if we can show:

$$\mathrm{Iso} : [0, \sqrt{2}-1) \to [(3/2)(2\pi^2)^{-1/4}, 1), \quad \mathrm{Iso}(a) := v\big(i_{(a,0,0)}(T_{\sqrt{2}})\big) \tag{1.7}$$

is a bijection. If so, then each $v_0 \in [(3/2)(2\pi^2)^{-1/4}, 1)$ corresponds to one and only one Clifford torus, namely $i_{(\mathrm{Iso}^{-1}(v_0),0,0)}(T_{\sqrt{2}})$, with isoperimetric ratio v_0, which must be the unique solution of the genus 1 Canham problem with v_0 as the constrained isoperimetric ratio.

To prove that Iso is a bijection, it suffices to show that Iso is monotonic increasing and

$$\lim_{a \to \sqrt{2}-1} \mathrm{Iso}(a) = 1. \tag{1.8}$$

In Section 3, we establish Theorem 3.1, which is a more general version of (1.8).

III. To prove that Iso is monotonic increasing, we venture into the realm of special functions. We make the observation that the area and enclosing volume of the cyclides in (1.6), denoted by $A(a)$ and $V(a)$, can be extended analytically to the disc $\{z : |z| < \sqrt{2}-1\}$ on the complex plane. Moreover, the coefficients $(a_n)_{n\geqslant 0}$ and $(v_n)_{n\geqslant 0}$ of their power series at $z = 0$ are holonomic, or P-recursive, sequences, i.e. they satisfy linear recurrences with polynomial coefficients. We work out explicitly these P-recurrences in Section 4.

Since $\mathrm{Iso}^2(a)/(36\pi) = V^2(a)/A^3(a)$, Iso is monotonic increasing iff the logarithm of the right-hand side is. But then we have

$$\frac{d}{da} \ln \frac{V^2(a)}{A^3(a)} = \frac{2V'(a)A(a) - 3V(a)A'(a)}{V(a)A(a)},$$

so Iso is monotonic increasing iff $2V'(a)A(a) - 3V(a)A'(a) > 0$ on $[0, \sqrt{2}-1)$. The fact that $A(z)$ and $V(z)$ are holonomic implies that $D(z) := 2V'(z)A(z) - 3V(z)A'(z)$ is also holonomic; the coefficients $(d_n)_{n\geqslant 0}$ of the power series of $D(z)$ at $z = 0$ follows the P-recurrence (4.7) derived in Section 4.

The monotonicity of Iso follows if all the terms defined by the P-recurrence (4.7) are positive.

*IV. Prove that all terms defined by the P-recurrence (4.7) are positive.

This last step is out of the scope of this paper. It is well-known to experts in holonomic functions that positivity of a P-recurrence is difficult to establish when its characteristics polynomial has a non-simple dominant root, as is the case of (4.7). We can, however, use the existing tools to check that the sequence is *eventually positive*; see Section 4 and the remarks in Section 5.

To summarize, the result of this article is:

Proposition 1.2. *Assuming the positivity of the P-recurrence (4.7), Conjecture 1.1(iii) holds, i.e. for every isoperimetric ratio $v_0 \in \big[(3/2)(2\pi^2)^{-1/4}, 1\big)$, there is a unique Möbius transformation of $T_{\sqrt{2}}$ with isoperimetric ratio v_0.*

Steps I-III are carried out in the next three sections.

2 Step I: Non-homothetic Clifford tori

Let $T_R := \{(R+\cos v)\cos u, (R+\cos v)\sin u, \sin v) : u, v \in [0, 2\pi]\}$, a torus with major radius $R \in (1, \infty)$, minor radius 1, and the z-axis as the axis of revolution. Let $i_{(x,y,z)}$ be the inversion map about the unit sphere centered at (x, y, z) of $\mathbb{R}^3$. Our goal is to characterize all the Euclidean shapes of the Clifford tori, i.e. we would like to find a parametrization of the 'shape space'

$$\big\{i_{(x,y,z)}(T_{\sqrt{2}}) : (x, y, z) \in \mathbb{R}^3 \backslash T_{\sqrt{2}}\big\} \Big/ \mathrm{Hom}(3). \tag{2.1}$$

Here '/Hom(3)' means we identify two point sets if they can be transformed from one to another by a homothety in $\mathbb{R}^3$. Since we are primarily interested in Euclidean shapes here, we avoid sphere inversions centered at points on T_R itself. To help us gain a better understanding of the underlying structure, we also study the more general shape space

$$\big\{i_{(x,y,z)}(T_R) : R > 1,\ (x, y, z) \in \mathbb{R}^3 \backslash T_R\big\} \Big/ \mathrm{Hom}(3). \tag{2.2}$$

Maxwell's characterization of a cyclide. It is well-known that any (torodial) cyclide $\mathfrak{C}$ has two orthogonal planes of mirror symmetry; see, for example, [20, 3, 5]. We make the observation that the Euclidean shape of a toroidal cyclide $\mathfrak{C}$ is uniquely determined by certain measurements of the cross section of $\mathfrak{C}$ with either one of the two symmetry planes.

We use Maxwell's characterization of cyclides [20, 3, 5]: any cyclide $\mathfrak{C}$ is the envelope of all the spheres centered at the points P on a given ellipse $\mathcal{E}$ with radii $r(P)$, $P \in \mathcal{E}$, satisfying $r(P) + \overline{FP} = L$, where F is one of the foci of $\mathcal{E}$ and L is a constant in a suitable range. We can think of L as the length of a taut string attached in one end to F; the string slides smoothly on $\mathcal{E}$ and traces out spheres with the other end. See Figure 2. Under this characterization, $\mathfrak{C}$ is a torodial cyclide if and only if

$$a > L - a > f,$$

where a, f and L are the major radius of $\mathcal{E}$, the focal length of $\mathcal{E}$, and the length of the string, respectively. Moreover, the Euclidean shape of $\mathfrak{C}$ can be characterized by the ratio $a : f : L$.[2]

The major axis of $\mathcal{E}$ lies on the intersecting line of the two symmetry planes of $\mathfrak{C}$. In the following, P_1 refers to the symmetry plane where $\mathcal{E}$ lies, whereas P_2 ($\perp P_1$) refers to the other symmetry plane. The cross section $\mathfrak{C} \cap P_1$ consists of two circles **exterior to each other**, whereas the cross section $\mathfrak{C} \cap P_2$ consists of two circles with **one lying inside the other** (see Figure 2).

Denote the radii of the two circles in $\mathfrak{C} \cap P_1$ by r_1 and r_2 and the distance between the two centers by d (see Figure 2). Similarly, let $\tilde{r}_1$ and $\tilde{r}_2$ be the radii of the two circles in $\mathfrak{C} \cap P_2$ and $\tilde{d}$ be the distance between the two centers. By convention, $r_1 \geqslant r_2$, $\tilde{r}_1 \geqslant \tilde{r}_2$. The three sets of measurements (r_1, r_2, d), $(\tilde{r}_1, \tilde{r}_2, \tilde{d})$ and (a, f, L) of a cyclide $\mathfrak{C}$ are related by the following equations:

$$a = \frac{d}{2},\quad f = \frac{r_1 - r_2}{2},\quad L = \frac{d + r_1 + r_2}{2}. \tag{2.3}$$

$$\tilde{r}_1 = \frac{d + (r_1 + r_2)}{2},\quad \tilde{r}_2 = \frac{d - (r_1 + r_2)}{2},\quad \tilde{d} = r_1 - r_2. \tag{2.4}$$

Since the maps $(a, f, L) \mapsto (r_1, r_2, d)$ and $(r_1, r_2, d) \mapsto (\tilde{r}_1, \tilde{r}_2, \tilde{d})$ are linear isomorphisms, we conclude that:

[2] This already explains why the shape space (2.2) is two-dimensional.

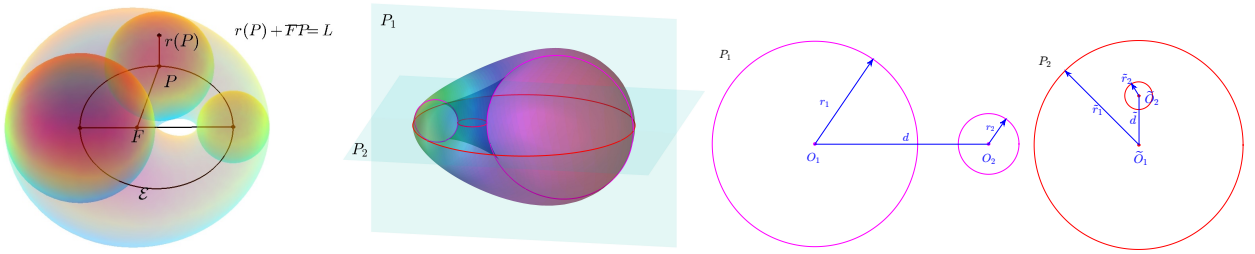

(a) (b) (c) $i_{(x,y,z)}(T_R) \cap P_1$ (d) $i_{(x,y,z)}(T_R) \cap P_2$

Figure 2: (a) Maxwell's characterization of a torodial cyclide, (b) Two planes of mirror symmetry, (c)-(d) Cross sections of $i_{(x,y,z)}(T_R)$ with P_1 and P_2

Lemma 2.1. *Each of the three ratios*

$$a : f : L, \quad r_1 : r_2 : d \quad \textit{and} \quad \tilde{r}_1 : \tilde{r}_2 : \tilde{d}$$

determines the Euclidean shape of the cyclide $\mathfrak{C}$.

For any $\varrho > 0$, let $\mathcal{C}(\varrho) = \mathcal{C}(\varrho; R)$ be the circle in the ϱ-z plane with a diameter connecting $(\varrho, 0)$ and $\big((R^2-1)/\varrho, 0\big)$; see Figure 3. By convention, $\mathcal{C}(0) = \mathcal{C}(\infty)$ is the z-axis. In general, we have

$$C(\varrho) = C((R^2-1)/\varrho).$$

These circles on the plane can be extended to the following tori in 3-D:

$$\mathcal{T}(\varrho) := \mathcal{T}(\varrho; R) := \{(\rho\cos(\theta), \rho\sin(\theta), z) : (\rho, z) \in \mathcal{C}(\varrho),\ \theta \in [0, 2\pi]\}\,. \tag{2.5}$$

For any fixed R, the torus $\mathcal{T}(\varrho)$ lies completely outside, on, or inside the torus T when $\varrho \in [0, R-1) \cup (R+1, \infty]$, $\varrho = R \mp 1$, or $\varrho \in (R-1, R+1)$, respectively. In particular, $\mathcal{T}(R \pm 1; R) = T_R$. On the ρ-z plane, these correspond to the red, green and blue circles in Figure 3. While the one-parameter family of circles

$$\Big\{\mathcal{C}(\varrho) : \varrho \in [0, \sqrt{R^2-1}]\Big\}$$

partitions the ρ-z plane,[3] the corresponding one-parameter family of tori

$$\Big\{\mathcal{T}(\varrho) : \varrho \in [0, \sqrt{R^2-1}]\Big\}$$

partitions $\mathbb{R}^3$. We shall see that how these circles and tori characterize the shape spaces (2.1) and (2.2).

Theorem 2.2. *For any fixed* $R \in (1, \infty)$ *and* $\varrho \in [0, \infty] \backslash \{R-1, R+1\}$, *all the cyclides in*

$$\Big\{i_{(x,y,z)}(T_R) : \quad (x, y, z) \in \mathcal{T}(\varrho; R)\Big\}, \tag{2.6}$$

are homothetic in $\mathbb{R}^3$.

[3] Any (ρ, z), $\rho > 0$, lies on the circle $\mathcal{C}(\varrho^+) = \mathcal{C}(\varrho^-)$, where

$$\varrho^{\pm} = \frac{(\rho^2 + z^2 + R^2 - 1) \pm \sqrt{(\rho^2 + z^2 + R^2 - 1)^2 - 4\rho^2(R^2-1)}}{2\rho}.$$

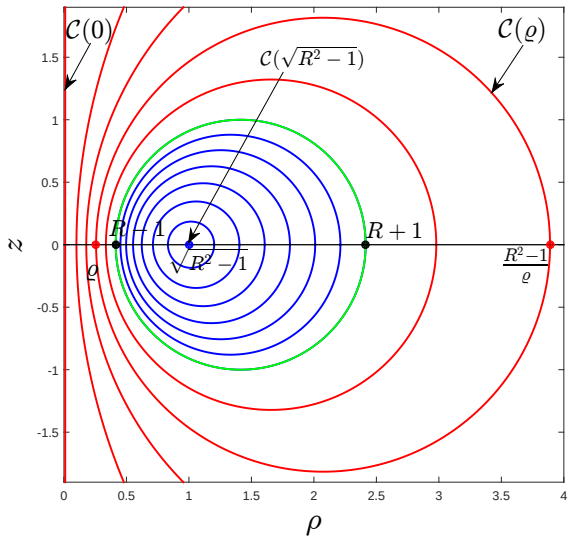

Figure 3: $\mathcal{C}(\varrho)$ for various values of $\varrho \in (0, R-1)$ (in red) and $\varrho \in (R-1, \sqrt{R^2-1})$ (in blue). Note that $\mathcal{C}(\varrho) = \mathcal{C}((R^2-1)/\varrho)$ and $\mathcal{C}(\sqrt{R^2-1})$ degenerates into a point.

Proof: We divide the proof into 3 steps.

1° By rotational symmetry, the shape of $i_{(\rho\cos(\theta),\rho\sin(\theta),z)}(T_R)$ is independent of θ. So it suffices to prove that all cyclides of the form

$$i_{(\rho,0,z)}(T_R), \quad (\rho, z) \in \mathcal{C}(\varrho),$$

are homothetic.

By Lemma 2.1, the Euclidean shape of $i_{(\rho,0,z)}(T_R)$ is determined by the measurements of its cross section at the x-z plane. Denote by P the x-z plane and $\pi : \mathbb{R}^3 \to \mathbb{R}^2$ be the ortho-projection map onto P. Note that

$$\pi\left(i_{(\rho,0,z)}(T_R) \cap P\right) = i_{(\rho,z)}\left(\pi(T_R \cap P)\right). \tag{2.7}$$

Here $i_{(\rho,z)}$ stands for the circle inversion map in 2-D with respect to the unit circle centered at (ρ, z). Note that P is a symmetry plane of the cyclides (2.7) and that the cross section (2.7) consists of a circle pair. Therefore, by (the implication of) Lemma 2.1, it suffices to check that these circle pairs corresponding to different $(\rho, z) \in \mathcal{C}(\varrho)$ are all homothetic. We have reduced the problem into one of plane geometry.

2° We recall a well-known fact about circle inversion. If we invert two circles centered at $(x_1, 0)$ and $(x_2, 0)$ with radii r_1 and r_2 about a circle centered anywhere on the line

$$\left\{(x_{ra}, y) \;\middle|\; x_{ra} = \frac{(x_2^2 - x_1^2) + (r_1^2 - r_2^2)}{2(x_2 - x_1)}\right\}, \tag{2.8}$$

the resulting circle pair is homothetic to the original circle pair. This line is called the *radical axis* of the circle pair; see Figure 4.

We first determine the image of the circle pair $\pi(T_R \cap P)$ under the circle inversion $i_{(\varrho,0)}$. The circle pairs in $\pi(T_R \cap P)$ consist of two unit circles with diameters A_1B_1 and A_2B_2, both on the x-axis, with $A_1 = (R-1, 0)$, $B_1 = (R+1, 0)$, $A_2 = (-(R+1), 0)$ and $B_2 = (-(R-1), 0)$. The images of A_1, B_1, A_2, B_2 under $i_{(\varrho,0)}$, denoted by A_1', B_1', A_2', B_2', again lie on the x-axis and form the diameters $A_1'B_1'$, $A_2'B_2'$ of circle pair in $i_{(\varrho,0)}(\pi(T_R \cap P))$.

- When $\varrho \in (0, R-1)$, $B_2' < A_2' < B_1' < A_1'$.

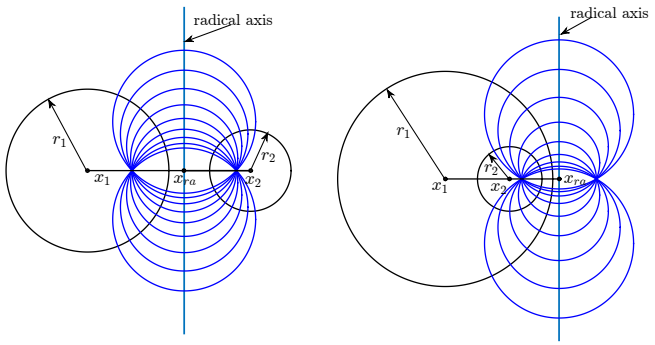

Figure 4: Radical Axis of a circle pair: (left) two circles exterior to each other; (right) one circle lying inside the other. The blue circles meet the circle pair orthogonally.

- When $\varrho \in (R+1, \infty)$, $B_1' < A_1' < B_2' < A_2'$.
- When $\varrho \in (R-1, R+1)$, $A_1' < B_2' < A_2' < B_1'$.

[4] In the first two cases, the circle pair are exterior of each other, as in Figure 4(a); in the last case, one circle lies inside the other, as in Figure 4(b). In any case, the resulting circle pair has the following radii and centers:

$$\begin{aligned} \mathfrak{r}_1 &= \frac{|A_1' - B_1'|}{2} = \frac{1}{|(\varrho - R)^2 - 1|}, \quad \mathfrak{r}_2 = \frac{|A_2' - B_2'|}{2} = \frac{1}{(\varrho + R)^2 - 1} \\ O_1 &= \frac{A_1' + B_1'}{2} = \Big(\varrho - \frac{\varrho - R}{(\varrho - R)^2 - 1}, 0\Big), \quad O_2 = \frac{A_2' + B_2'}{2} = \Big(\varrho - \frac{\varrho + R}{(\varrho + R)^2 - 1}, 0\Big). \end{aligned} \tag{2.9}$$

By (2.8) and (2.9), the radical axis of the circle pair $i_{(\varrho,0)}\left(\pi(T_R \cap P)\right)$ is given by $\{(\rho_{ra}, z) : z \in \mathbb{R}\}$ where

$$\rho_{ra} = \varrho - \frac{\varrho}{\varrho^2 + 1 - R^2}.$$

Now the circle pairs in

$$\Big\{ i_{(\rho_{ra},z)} \circ i_{(\varrho,0)}(\pi(T_R \cap P)) : \ z \in \mathbb{R} \Big\} \tag{2.10}$$

are all homothetic. The theorem is proved if we show that every circle pair in $\Big\{ i_{(\rho,z)}(\pi(T_R \cap P)) : \ (\rho, z) \in \mathcal{C}(\varrho) \Big\}$ is homothetic to some circle pair in (2.10). We do so in the last step of the proof.

3° Since an arbitrary composition of inversions can be written as a composition of an inversion (of radius 1) with a homothety (see [1, Page 92]),

$$i_{(\rho_{ra},z)} \circ i_{(\varrho,0)} = \mathcal{H} \circ i_{(\rho_1,z_1)}. \tag{2.11}$$

We can determine (ρ_1, z_1) using the following properties of an inversion i_O to find (ϱ_1, z_1): $i_O(O) = \infty$, $i_O(\infty) = O$, and $i_O(Q_1) = Q_2 \Leftrightarrow i(Q_2) = Q_1$. By the first property,

$$i_{(\rho_{ra},z)} \circ i_{(\varrho,0)}(\rho_1, z_1) = \mathcal{H} \circ i_{(\rho_1,z_1)}(\rho_1, z_1) = \infty.$$

By the second property,

$$i_{(\varrho,0)}(\rho_1, z_1) = (\rho_{ra}, z).$$

[4] Here and below, $A < B$ simply means A is on the left of B for two points A and B are on the first axis of $\mathbb{R}^2$.

By the third property,

$$(\rho_1, z_1) = i_{(\varrho,0)}(\rho_{ra}, z),$$

This means the set of all (ρ_1, z_1) in (2.11) is the image of the line $\{(\rho_{ra}, z)|z \in \mathbb{R}\}$ under the inversion $i_{(\varrho,0)}$, which is a circle. By symmetry, this circle has a diameter on the x-axis. One end of the diameter is $i_{(\varrho,0)}((\rho_{ra}, \infty)) = (\varrho, 0)$, and the other end is $i_{(\varrho,0)}((\varrho_{ra}, 0)) = \frac{R^2-1}{\varrho}$. The circle is $\mathcal{C}(\varrho)$. ■

In virtue of Theorem 2.2, we use the shorthand notation

$$i_\varrho(T_R)$$

to represent the common Euclidean shape of the cyclides in (2.6). Formally, $i_\varrho(T_R)$ is an element in the shape space (2.2).

To further analyze the shape $i_\varrho(T_R)$, by Lemma 2.1 and Theorem 2.2, it suffices to analyze the ratio $r_1 : r_2 : d$ of the cross-section of $i_{(\varrho,0,0)}(T_R)$ at its P_1 symmetry plane.

Lemma 2.3. *For any $R \in (1, \infty)$, the P_1 cross section of $\mathfrak{C} = i_{(\varrho,0,0)}(T_R)$ has the following measurements:*

(i) when $\varrho \in [0, R-1)$ (corresponding to the red circles in Figure 3(a)), the P_1 symmetry plane of $\mathfrak{C}$ is the x-z plane, and

$$r_1 : r_2 : d = \lambda : 1 : \sqrt{(\lambda-1)^2 + 4\lambda R^2}, \quad \text{where } \lambda = \frac{r_1}{r_2} = \frac{(\varrho+R)^2 - 1}{(\varrho-R)^2 - 1} \in [1, \infty). \tag{2.12}$$

(ii) when $\varrho \in \left(R-1, \sqrt{R^2-1}\right]$ (corresponding to the blue circles in Figure 3(a)), the P_1 symmetry plane of $\mathfrak{C}$ is the x-y plane, and

$$r_1 : r_2 : d = \lambda : 1 : \sqrt{(\lambda-1)^2 + 4\lambda \frac{R^2}{R^2-1}}, \text{ where } \lambda = \frac{r_1}{r_2} = \frac{(R-1)[(R+1)^2 - \varrho^2]}{(R+1)[\varrho^2 - (R-1)^2]} \in [1, \infty). \tag{2.13}$$

Proof: The first two steps of the proof of Theorem 2.2 imply that

$$P, \text{the } x\text{-}z \text{ plane, is } \begin{cases} \text{the } P_1 \text{ symmetry plane of } \mathfrak{C} \text{ when } \varrho \in [0, R-1) \\ \text{the } P_2 \text{ symmetry plane of } \mathfrak{C} \text{ when } \varrho \in \left(R-1, \sqrt{R^2-1}\right] \end{cases}.$$

In the first case, $\mathfrak{r}_i$ and O_i in (2.9) are such that $\mathfrak{r}_1 > \mathfrak{r}_2$ and $O_2 < O_1$, and they give the (r_1, r_2, d) measurements of $\mathfrak{C}$:

$$r_1 = \frac{1}{(\varrho-R)^2 - 1}, \quad r_2 = \frac{1}{(\varrho+R)^2 - 1}, \quad d = \frac{\varrho+R}{(\varrho+R)^2 - 1} - \frac{\varrho-R}{(\varrho-R)^2 - 1}. \tag{2.14}$$

In the second case, we also have $\mathfrak{r}_1 > \mathfrak{r}_2$ but now $O_1 < O_2$, and they give the $(\tilde{r}_1, \tilde{r}_2, \tilde{d})$ measurements of $\mathfrak{C}$:

$$\tilde{r}_1 = \frac{1}{1 - (\varrho-R)^2}, \quad \tilde{r}_2 = \frac{1}{(\varrho+R)^2 - 1}, \quad \tilde{d} = -\frac{\varrho+R}{(\varrho+R)^2 - 1} + \frac{\varrho-R}{(\varrho-R)^2 - 1}.$$

By (2.4), we can convert the $(\tilde{r}_1, \tilde{r}_2, \tilde{d})$ measurements to the (r_1, r_2, d) measurements via $r_1 = (\tilde{r}_1 - \tilde{r}_2 + \tilde{d})/2$, $r_2 = (\tilde{r}_1 - \tilde{r}_2 - \tilde{d})/2$, $d = \tilde{r}_1 + \tilde{r}_2$, so

$$r_1 = \frac{R-1}{\varrho^2 - (R-1)^2}, \quad r_2 = \frac{R+1}{(R+1)^2 - \varrho^2}, \quad d = \frac{1}{(R+\varrho)^2 - 1} - \frac{1}{(R-\varrho)^2 - 1}. \tag{2.15}$$

By routine computations, (2.12) follows from (2.14) and (2.13) follows from (2.15). ■

Lemma 2.3 has an almost immediate consequence:

Theorem 2.4. *For any $R \in (1,\infty)$, $i_\varrho(T_R)$ is distinct for each $\varrho \in [0, R-1)$.*

- *If $R \neq \sqrt{2}$, then $i_\varrho(T_R)$ is distinct for each $\varrho \in [0, R-1) \cup (R-1, \sqrt{R^2-1}]$.*
- *If $R = \sqrt{2}$, then $\varrho > \sqrt{2}-1$ adds no new shape and hence the shape space (2.1) is in one-to-one correspondence with*

$$\left\{ i_\varrho(T_{\sqrt{2}}) : \varrho \in [0, \sqrt{2}-1) \right\}.$$

Proof: Recall the two expressions in Lemma 2.3 for $\lambda = r_1/r_2$ in the two intervals of ϱ. It is easy to check that both

$$\lambda_1 : [0, R-1) \to [1,\infty), \quad \lambda_1(\varrho) = \frac{(\varrho+R)^2-1}{(\varrho-R)^2-1}$$

and

$$\lambda_2 : \left(R-1, \sqrt{R^2-1}\right] \to [1,\infty), \quad \lambda_2(\varrho) = \frac{(R-1)[(R+1)^2-\varrho^2]}{(R+1)[\varrho^2-(R-1)^2]}$$

are bijections: simply check that λ_1 is monotonic increasing from 1 to ∞, and λ_2 is monotonic decreasing from ∞ to 1. As the $r_1 : r_2$ ratio of $i_\varrho(T_R)$ is distinct for different $\varrho \in [0, R-1)$, the first statement of the theorem is true. Likewise, $i_\varrho(T_R)$ is also distinct for each $\varrho \in (R-1, \sqrt{R^2-1}]$.

To show the statement in the first bullet, it remains to argue that for $\varrho_1 \in [0, R-1)$ and $\varrho_2 \in (R-1, \sqrt{R^2-1}]$, $i_{\varrho_1}(T_R) \neq i_{\varrho_2}(T_R)$. There are two cases:

1. If $\lambda_1(\varrho_1) \neq \lambda_2(\varrho_2)$, then $i_{\varrho_1}(T_R) \neq i_{\varrho_2}(T_R)$.
2. If $\lambda_1(\varrho_1) = \lambda_2(\varrho_2)$, then, by the expressions of the $r_2 : d$ ratio in Lemma 2.3, the $r_2 : d$ ratios of $i_{\varrho_1}(T_R)$ and $i_{\varrho_2}(T_R)$ are different exactly when $R^2 \neq \frac{R^2}{R^2-1}$. But

$$R^2 = \frac{R^2}{R^2-1} \iff R = \sqrt{2}.$$

So we also have $i_{\varrho_1}(T_R) \neq i_{\varrho_2}(T_R)$ in this case.

This argument proves the statement under the second bullet as well. ∎

The next two results characterize the bigger shape space (2.2); they are inspiring for us but technically we do not need them for this article. We omit the detailed proofs, which follow the same line of arguments as in that of Theorem 2.4.

Lemma 2.5. *For any $R \in (1,\infty)$, $\varrho \in [0, \sqrt{R^2-1}]$,*

$$i_\varrho(T_R) = i_{\varrho'}(T_{R'}) \quad \text{where} \quad (R', \varrho') = \frac{1}{\sqrt{R^2-1}}\left(R, \frac{\sqrt{R^2-1}-\varrho}{\sqrt{R^2-1}+\varrho}\right). \tag{2.16}$$

Theorem 2.6. *Let*

$$C_R := \begin{cases} \left[0, \sqrt{R^2-1}\right] \backslash \{R-1\} & \text{if } R \in (1, \sqrt{2}) \\ \left[0, \sqrt{2}-1\right) & \text{if } R = \sqrt{2} \end{cases}, \quad C := \bigcup_{R \in (1,\sqrt{2}]} \{(R,\varrho) : \varrho \in C_R\}.$$

Distinct elements in C correspond to distinct $i_\varrho(T_R)$ and the shape space (2.2) is in one-to-one correspondence with

$$\left\{ i_\varrho(T_R) : (R,\varrho) \in C \right\}.$$

Remark 2.7. Admittedly, our proof of Theorem 2.4 is very elementary given the extensive development in Möbius geometry; see, for example, [11, 12]. For instance, we use neither the usual representation of the Möbius group Möb(3) in $\mathbb{S}^3$ nor its linear representation in the Lorentz space $\mathbb{R}^{4,1}$. It is unclear to us if our proof can be shortened using the more modern techniques.

3 Step II: Rounding by sphere inversion

Theorem 3.1. *If S is a compact regular surface (with or without boundary) in $\mathbb{R}^3$ and $p \in S$, then*

$$\text{Area}(i_q(S)) \sim \frac{\pi}{|p-q|^2}, \quad q \to p, \quad \overline{pq} \perp T_pS. \tag{3.1}$$

If S is also closed and orientable (so S and $i_q(S)$ have enclosing volumes), then

$$\text{Volume}(i_q(S)) \sim \frac{\pi}{6|p-q|^3}, \quad q \to p, \quad \overline{pq} \perp T_pS, \tag{3.2}$$

and (consequently)

$$v(i_q(S)) = \frac{\text{Volume}(i_q(S))}{(4\pi/3)\left(\text{Area}(i_q(S))/(4\pi)\right)^{3/2}} \to 1, \quad q \to p, \quad \overline{pq} \perp T_pS. \tag{3.3}$$

Proof: Without loss of generality assume $p = (0,0,0)$ and T_pS is the x-y plane, and let ε be a small scalar representing the point $q = (0,0,\varepsilon)$ approaching the surface orthogonally at the origin. So the surface near p can be written as the graph of a smooth function $h(x,y)$, where $x^2+y^2 < R^2$ for some $R > 0$ and h has a vanishing linear approximation at the origin, i.e. $h(0,0) = 0 = \frac{\partial h}{\partial x}(0,0) = \frac{\partial h}{\partial y}(0,0)$, and so

$$h(x,y) = O(x^2+y^2), \quad |\nabla h(x,y)| = O(\sqrt{x^2+y^2}), \quad (x,y) \to (0,0). \tag{3.4}$$

Write $S_R := \{(x,y,h(x,y)) : x^2+y^2 < R^2\})$. By continuity, the area of $i_{(0,0,\varepsilon)}(S \backslash S_R)$ approaches that of $i_{(0,0,0)}(S \backslash S_R)$ as $\varepsilon \to 0$ and hence stays bounded for small ε. So it suffices to prove (3.1) with S replaced by S_R.

The conformal factor of $i_{\mathbf{a}}$ is $\lambda^2(\mathbf{a},\mathbf{x}) = 1/\|\mathbf{x}-\mathbf{a}\|^4$, i.e. $\langle di_{\mathbf{a}}|_{\mathbf{x}} v, di_{\mathbf{a}}|_{\mathbf{x}} w\rangle = \lambda^2(\mathbf{a},\mathbf{x})\langle v, w\rangle$. Therefore,

$$\begin{aligned} \text{Area}(i_{(0,0,\varepsilon)}(S_R)) &= \iint_{x^2+y^2<R^2} \frac{\sqrt{1+|\nabla h(x,y)|^2}}{[x^2+y^2+(h(x,y)-\varepsilon)^2]^2}\, dxdy \\ &= \int_0^{2\pi} \left[\int_0^R \frac{\sqrt{1+|\nabla h(re^{i\theta})|^2}}{[r^2+(\varepsilon - h(re^{i\theta}))^2]^2}\, rdr \right] d\theta. \end{aligned} \tag{3.5}$$

Let $r_*(\varepsilon) = |\varepsilon|^\alpha$ for any $\alpha \in (1/2, 1)$ so that

$$\text{(i) } |\varepsilon| = o(r_*(\varepsilon)) \quad \text{and} \quad \text{(ii) } r_*(\varepsilon) = o(|\varepsilon|^{1/2}), \quad \text{as } \varepsilon \to 0. \tag{3.6}$$

We then split the inner integral in (3.5) into $\int_0^{r_*(\varepsilon)} + \int_{r_*(\varepsilon)}^R$; define

$$J(\varepsilon) := \int_0^{2\pi} \int_0^{r_*(\varepsilon)} \frac{\sqrt{1+|\nabla h(re^{i\theta})|^2}}{[r^2+(\varepsilon - h(re^{i\theta}))^2]^2}\, rdrd\theta, \quad K(\varepsilon) := \int_0^{2\pi} \int_{r_*(\varepsilon)}^K \frac{\sqrt{1+|\nabla h(re^{i\theta})|^2}}{[r^2+(\varepsilon - h(re^{i\theta}))^2]^2}\, rdrd\theta.$$

We shall prove (3.1) by showing that the former integral is asymptotically equivalent to $\varepsilon^{-2}/2$ and the latter grows slower than ε^{-2}.

For $J(\varepsilon)$, we compare it with the special case when $h \equiv 0$. By (3.4), there exists a constant $C > 0$, independent of r and θ, such that

$$|\nabla h(re^{i\theta})|^2, \ |h(re^{i\theta})| \leqslant Cr^2.$$

For $r \in [0, r_*(\varepsilon)]$, $r^2 \leqslant r_*(\varepsilon)^2 = o(|\varepsilon|)$ by (3.6)(ii), so $\varepsilon - h(re^{i\theta}) \sim \varepsilon$. Also, $1 + |\nabla h(re^{i\theta})|^2 \sim 1$. From this it is easy to see that

$$J(\varepsilon) \sim \int_0^{2\pi} \int_0^{r_*(\varepsilon)} \frac{r}{[r^2+\varepsilon^2]^2}\, drd\theta. \tag{3.7}$$

The right-hand side is $J(\varepsilon)$ in the case of $h \equiv 0$, whose asymptotic can be easily determined:

$$\int_0^{2\pi}\int_0^{r_*(\varepsilon)} \frac{r}{[r^2+\varepsilon^2]^2}\,dr d\theta = \frac{2\pi}{\varepsilon^2}\int_0^{r_*(\varepsilon)/\varepsilon} \frac{s\,ds}{(1+s^2)^2} = \frac{2\pi}{\varepsilon^2}\left[\frac{1}{2} - \frac{1}{2(1+(r_*(\varepsilon)/\varepsilon)^2)}\right] \sim \frac{\pi}{\varepsilon^2},\quad \varepsilon\to 0. \tag{3.8}$$

In the last step above, we used (3.6)(i).

For $K(\varepsilon)$, note that ∇h is bounded on a compact set, so

$$\begin{aligned} K(\varepsilon) = \int_0^{2\pi}\int_{r_*(\varepsilon)}^{R} \frac{\sqrt{1+|\nabla h(re^{i\theta})|^2}}{[r^2+(\varepsilon-h(re^{i\theta}))^2]^2}\,r dr d\theta &\leqslant 2\pi\int_{r_*(\varepsilon)}^{R}\frac{C}{[r^2]^2}\,r dr \\ &\leqslant 2\pi C\int_{r_*(\varepsilon)}^{\infty} r^{-3}dr = \pi C r_*(\varepsilon)^{-2} = o(\varepsilon^{-2}). \end{aligned}$$

In the last step above, we again used (3.6)(i).

We have completed the proof of (3.1).

Let B be a ball whose boundary is tangent to S at p and lies inside of S, so $\mathrm{Volume}(B) \leqslant \mathrm{Volume}(S)$ and also

$$\mathrm{Volume}(i_q(B)) \leqslant \mathrm{Volume}(i_q(S)).$$

As before, write $|p-q| = \varepsilon$. Since $i_q(B)$ is a ball with diameter $\sim 1/\varepsilon$,

$$\mathrm{Volume}(i_q(B)) \sim \frac{4\pi}{3}\left(\frac{1}{2\varepsilon}\right)^3 = \frac{\pi}{6\varepsilon^3},\quad \varepsilon\to 0.$$

So $\mathrm{Volume}(i_q(S))$ grows at least as fast as $\pi/(6\varepsilon^3)$. By the first part of the theorem and the isoperimetric inequality, $\mathrm{Volume}(i_q(S))$ cannot grow faster than $\pi/(6\varepsilon^3)$, and (3.2) is proved. ∎

Remark 3.2. We thank I. Pinelis for the help in analyzing the asymptotic of the area integral (3.5); see https://mathoverflow.net/questions/353648/asymptotic-of-an-area-integral.

4 Step III: Reduction to P-recurrence

In this section we express by P-recurrences the surface area and enclosing volume of $i_{\mathbf{a}}(T_{\sqrt{2}})$, where $\mathbf{a} = [a,0,0]^T$, $a \in [0, \sqrt{2}-1)$, which are the same as those of $\mathrm{SCT}_{\mathbf{a}}(T_{\sqrt{2}})$. (Recall $i(T_{\sqrt{2}}) = T_{\sqrt{2}}$.) From these, an associated P-recurrence related to the isoperimetric ratio of $i_{\mathbf{a}}(T_{\sqrt{2}})$ will also be derived.

4.1 Area and volume integrals

The conformal factor of a special conformal transformation $\mathrm{SCT}_{\mathbf{a}} := i\circ t_{\mathbf{a}}\circ i$ is

$$\boxed{\lambda^2(\mathbf{a},\mathbf{x}) = \frac{1}{(1+2\langle\mathbf{a},\mathbf{x}\rangle + \langle\mathbf{a},\mathbf{a}\rangle\langle\mathbf{x},\mathbf{x}\rangle)^2},}$$

i.e. $\langle dS_{\mathbf{a}}|_{\mathbf{x}} v, dS_{\mathbf{a}}|_{\mathbf{x}} w\rangle = \lambda^2(\mathbf{a},\mathbf{x})\langle v, w\rangle$. So the area and enclosing volume of $\mathrm{SCT}_{[a,0,0]}(T_{\sqrt{2}})$ are given by

$$A(a) = \int_0^{2\pi}\int_0^{2\pi} Q(a;\mathbf{x})^{-2}\,d\mathrm{Area}(u,v), \quad V(a) = \int_0^1\int_0^{2\pi}\int_0^{2\pi} Q(a;\mathbf{x})^{-3}\,d\mathrm{Vol}(u,v,r),$$

where

$$Q(a;\mathbf{x}) := \frac{1}{\lambda([a,0,0]^T,\mathbf{x})} = 1 + 2\mathbf{x}_1 a + \|\mathbf{x}\|^2 a^2,$$

$$\mathbf{x}(u,v,r) = \Big[\big(\sqrt{2}+r\sin(v)\big)\cos(u),\ \big(\sqrt{2}+r\sin(v)\big)\sin(u),\ r\cos(v)\Big],\quad u,v\in[0,2\pi],\quad r\in[0,1],$$

$$d\mathrm{Area}(u,v) = (\sqrt{2}+\sin(v))\,du\,dv,\quad d\mathrm{Vol}(u,v,r) = r(\sqrt{2}+r\sin(v))\,du\,dv\,dr.$$

Notice also that

$$\langle\mathbf{x},\mathbf{x}\rangle = \|\mathbf{x}\|^2 = 2 + r^2 + 2\sqrt{2}r\sin(v).$$

4.2 Holomorphic extension

The integral definitions of A and V above extend from the interval $[0, \sqrt{2}-1)$ to a holomorphic function on the open disk

$$D := \{z \in \mathbb{C} : |z| < \sqrt{2}-1\}.$$

To see this, note that the roots of $Q(z;\mathbf{x})$, viewed as a quadratic polynomial in z, can be expressed as

$$\frac{-\mathbf{x}_1 \pm i\sqrt{\mathbf{x}_2^2+\mathbf{x}_3^2}}{\|\mathbf{x}\|^2},$$

so their moduli are both $1/\|\mathbf{x}\|$. But $\mathbf{x}$ is a point in the boundary or interior of the solid torus T, so $\|\mathbf{x}\| \in [\sqrt{2}-1, \sqrt{2}+1]$, which is equivalent to $1/\|\mathbf{x}\| \in [\sqrt{2}-1, \sqrt{2}+1]$. This means

$$Q(z;\mathbf{x}) \neq 0, \ \ \forall\, z \in D, \ \ \mathbf{x} \in T.$$

Therefore $Q(z;\mathbf{x})^{-L}$, $L = 2$ or 3, is holomorphic in the first argument and continuous in the second. A standard argument in complex analysis shows that A and V, defined based on the integrals in (4.1), extend to holomorphic functions on D.

So from now on, we write $A(z)$ and $V(z)$ instead of $A(a)$ and $V(a)$.

4.3 Power series at $z = 0$

Since A and V are even functions, the odd power Taylor coefficients at $z = 0$ all vanish. Denote by a_j and v_j the coefficients of z^{2j} in the expansions of $A(z)$ and $V(z)$ at $z = 0$, respectively. An observation here is that

$$\begin{aligned}
\frac{d^n A}{dz^n}(0) &= \iint_{\partial T} \frac{d^n}{dz^n} Q(z;\mathbf{x}(u,v,1))^{-2}\Big|_{z=0} d\mathrm{Area}(u,v) \\
\frac{d^n V}{dz^n}(0) &= \iiint_{T} \frac{d^n}{dz^n} Q(z;\mathbf{x}(u,v,r))^{-3}\Big|_{z=0} d\mathrm{Vol}(u,v,r),
\end{aligned} \tag{4.1}$$

and, thanks to the evaluation at $z = 0$, the integrands above are *polynomials* in $\mathbf{x}_1$ and $\|\mathbf{x}\|^2$, hence are *trigonometric polynomials* in (u, v).

Using either (4.1) or the generalized binomial theorem to expand $Q(z;\mathbf{x})^{-L}$ into a power series of z, i.e.

$$Q(z;\mathbf{x})^{-L} = \sum_{n=0}^{\infty} \binom{n+L-1}{n} (-1)^n (2\mathbf{x}_1 z + \|\mathbf{x}\|^2 z^2)^n,$$

together with the identity (of Wallis' integrals):

$$\int_0^{2\pi} \cos^n(v)\, dv = \int_0^{2\pi} \sin^n(v)\, dv = \begin{cases} \frac{2\pi}{2^n}\binom{n}{n/2}, & n \text{ even} \\ 0, & n \text{ odd} \end{cases},$$

we have

$$\begin{aligned}
a_j &= \sum_{\ell=0}^{j} (-1)^{j-\ell}(j+\ell+1)\binom{j+\ell}{j-\ell} \int_0^{2\pi}\int_0^{2\pi} (2\mathbf{x}_1(u,v,1))^{2\ell} \|\mathbf{x}(u,v,1)\|^{2(j-\ell)} d\mathrm{Area}(u,v) \\
&= \sum_{\ell=0}^{j} (-1)^{j-\ell}(j+\ell+1)\binom{j+\ell}{j-\ell} 4^{\ell} \underbrace{\int_0^{2\pi} \cos^{2\ell}(u)\, du}_{=2\pi\binom{2\ell}{\ell}/4^{\ell}} \underbrace{\int_0^{2\pi} (\sqrt{2}+\sin(v))^{2\ell+1}(3+2\sqrt{2}\sin(v))^{j-\ell} dv}_{=\sum_{p=0}^{2\ell+1}\sum_{q=0}^{j-\ell}\binom{2\ell+1}{p}\sqrt{2}^{2\ell+1-p}\binom{j-\ell}{q}3^{j-\ell-q}(2\sqrt{2})^q \int_0^{2\pi}\sin^{p+q}(v)\, dv}.
\end{aligned}$$

So,

$$
\begin{aligned}
a_j &= \sqrt{2}\pi^2 \sum_{\ell=0}^{j} (-1)^{j-\ell}\,(j+\ell+1)\binom{j+\ell}{j-\ell,\ell,\ell}\,\alpha_{\ell,j},\\
\alpha_{\ell,j} &= 2^{\ell+2}3^{j-\ell}\underbrace{\sum_{p=0}^{2\ell+1}\sum_{q=0}^{j-\ell}}_{p+q=\text{even}}\binom{2\ell+1}{p}\binom{j-\ell}{q}\binom{p+q}{(p+q)/2}2^{(q-3p)/2}3^{-q}.
\end{aligned}
\tag{4.2}
$$

Similarly,

$$
\begin{aligned}
v_j &= \sum_{\ell=0}^{j}(-1)^{j-\ell}\,\frac{(j+\ell+1)(j+\ell+2)}{2}\binom{j+\ell}{j-\ell}\int_0^1\int_0^{2\pi}\int_0^{2\pi}(2\mathbf{x}_1(u,v,r))^{2\ell}\|\mathbf{x}(u,v,r)\|^{2(j-\ell)}d\mathrm{Vol}(u,v,r)\\
&= \sum_{\ell=0}^{j}(-1)^{j-\ell}\,\frac{(j+\ell+1)(j+\ell+2)}{2}\binom{j+\ell}{j-\ell}4^{\ell}\underbrace{\int_0^{2\pi}\cos^{2\ell}(u)\,du}_{=2\pi\binom{2\ell}{\ell}/4^{\ell}}\times\\
&\qquad\qquad \underbrace{\int_0^1\int_0^{2\pi} r(\sqrt{2}+r\sin(v))^{2\ell+1}(2+r^2+2\sqrt{2}r\sin(v))^{j-\ell}dvdr.}_{\sum_{p=0}^{2\ell+1}\sum_{q=0}^{j-\ell}\binom{2\ell+1}{p}\sqrt{2}^{2\ell+1-p}\binom{j-\ell}{q}(2\sqrt{2})^q\int_0^{2\pi}\sin^{p+q}(v)\,dv\int_0^1 r^{p+q+1}(2+r^2)^{j-\ell-q}\,dr}
\end{aligned}
$$

So,

$$
\begin{aligned}
v_j &= \sqrt{2}\pi^2\sum_{\ell=0}^{j}(-1)^{j-\ell}\,(j+\ell+1)(j+\ell+2)\binom{j+\ell}{j-\ell,\ell,\ell}\,\nu_{\ell,j},\\
\nu_{\ell,j} &= 2^{\ell+1}\underbrace{\sum_{p=0}^{2\ell+1}\sum_{q=0}^{j-\ell}}_{p+q=\text{even}}\binom{2\ell+1}{p}\binom{j-\ell}{q}\binom{p+q}{(p+q)/2}2^{(q-3p)/2}\eta_{p,q,\ell,j},\\
\eta_{p,q,\ell,j} &= \int_0^1 r^{p+q+1}(2+r^2)^{j-\ell-q}\,dr = \sum_{k}^{j-\ell-q}\binom{j-\ell-q}{k}\frac{2^{j-\ell-q-k}}{2k+p+q+2}.
\end{aligned}
\tag{4.3}
$$

And we have the following power series:

$$
\begin{aligned}
\frac{1}{\sqrt{2}\pi^2}A(z) &= 4+52\,z^2+477\,z^4+3809\,z^6+\frac{451625}{16}\,z^8+\cdots\\
\frac{1}{\sqrt{2}\pi^2}V(z) &= 2+48\,z^2+\frac{1269}{2}\,z^4+6600\,z^6+\frac{1928025}{32}\,z^8+\cdots
\end{aligned}
$$

By the expressions (4.2)-(4.3), $\frac{1}{\sqrt{2}\pi^2}a_n$, $\frac{1}{\sqrt{2}\pi^2}v_n$ are rational.

4.4 Isoperimetric Ratio

To show that the isoperimetric ratio of $\mathrm{SCT}_{[a,0,0]}(T_{\sqrt{2}})$ is monotonic increasing in $a\in[0,\sqrt{2}-1)$, it suffices to show

$$
\Delta(a) := \frac{d}{da}\ln\frac{V(a)^2}{A(a)^3} = 2\frac{V'(a)}{V(a)}-3\frac{A'(a)}{A(a)} > 0,\quad \text{or}\quad 2V'(a)A(a)-3V(a)A'(a)>0.
$$

It happens that $\Delta(a)$ is proportional to the distance between the area and volume centers of the cyclide $\mathrm{SCT}_{[a,0,0]}(T)$. Precisely, $\Delta(a)=12\big[\mathbf{x}^A(a)-\mathbf{x}^V(a)\big]$ where $\mathbf{x}^A(a)$ and $\mathbf{x}^V(a)$ are the first coordinates of the area and volume centers of $\mathrm{SCT}_{[a,0,0]}(T_{\sqrt{2}})$, respectively. This follows from the observation that $(\mathrm{SCT}_{[a,0,0]}\circ\mathbf{x})_1=\frac{1}{2}Q'(a;\mathbf{x})/Q(a;\mathbf{x})$.

By the Taylor expansions of $A(a)$ and $V(a)$, we have

$$\begin{aligned}&\frac{1}{2\pi^4}(2V'(a)A(a)-3V(a)A'(a))\\&=\sum_k\Big[\underbrace{2(v_1a_k+2v_2a_{k-1}+\cdots+(k+1)v_{k+1}a_0)-3(a_1v_k+2a_2v_{k-1}+\cdots+(k+1)a_{k+1}v_0)}_{=:d_k}\Big]a^{2k+1}\\&=72\,a+1932\,a^3+31248\,a^5+\frac{790101}{2}\,a^7+\frac{17208645}{4}\,a^9+\cdots\end{aligned}\tag{4.4}$$

4.5 P-recurrence

The combinatorial expressions (4.2)-(4.3), together with the closure properties of holonomic sequences [27, 25, 15], show that $(a_n)_{n\geqslant 0}$ and $(v_n)_{n\geqslant 0}$ are P-recursive, i.e. they satisfy linear recurrences with polynomial coefficients. Equivalently, their generating functions, namely

$$\bar{A}(z)=\sum_{n\geqslant 0}a_nz^n,\quad \bar{V}(z)=\sum_{n\geqslant 0}v_nz^n,$$

are holonomic or D-finite, i.e. they satisfy linear differential equations with polynomial coefficients. The generating functions of $(a_n)_{n\geqslant 0}$ and $(v_n)_{n\geqslant 0}$ are related to the original area and volume functions $A(z)$ and $V(z)$ simply by $A(z)=\bar{A}(z^2)$ and $V(z)=\bar{V}(z^2)$. The generating function of the sequence $(d_k)_{k\geqslant 0}$, defined by (4.4), is given by

$$\bar{D}(z):=\sum_{n=0}^{\infty}d_nz^n=2\bar{V}'(z)\bar{A}(z)-3\bar{V}(z)\bar{A}'(z).$$

Since holonomic functions are closed under Hadamard product (hence differentiation), product, and linear combination, $(d_n)_{n\geqslant 0}$ is also holonomic.

Proposition 4.1. *The P-recurrences of $(a_n)_{n\geqslant 0}$, $(v_n)_{n\geqslant 0}$ and $(d_n)_{n\geqslant 0}$ are given by*

$$\sum_{i=0}^{3}p_i(n)a_{n+i}=0,\ \textit{where}\ \begin{bmatrix}p_0(n)\\p_1(n)\\p_2(n)\\p_3(n)\end{bmatrix}=\begin{bmatrix}-84&-136&-81&-21&-2\\399&730&484&137&14\\-474&-835&-529&-143&-14\\54&99&66&19&2\end{bmatrix}\begin{bmatrix}1\\n\\n^2\\n^3\\n^4\end{bmatrix}\tag{4.5}$$

$$\sum_{i=0}^{3}q_i(n)v_{n+i}=0,\ \textit{where}\ \begin{bmatrix}q_0(n)\\q_1(n)\\q_2(n)\\q_3(n)\end{bmatrix}=\begin{bmatrix}-252&-303&-136&-27&-2\\960&1384&730&167&14\\-1008&-1436&-748&-169&-14\\90&141&82&21&2\end{bmatrix}\begin{bmatrix}1\\n\\n^2\\n^3\\n^4\end{bmatrix}\tag{4.6}$$

$$\sum_{i=0}^{7}r_i(n)d_{n+i}=0,\ \textit{where}\ [r_0(n),r_1(n),\ldots,r_7(n)]^T=M[1,n,n^2,\ldots,n^7]^T,$$

$$M=\begin{bmatrix}-\frac{1630207404}{1529}&-\frac{3176073675}{3058}&-\frac{660587685}{1529}&-\frac{1216898711}{12232}&-\frac{167529251}{12232}&-\frac{626799}{556}&-\frac{7141}{139}&-1\\\frac{18219511026}{1529}&\frac{6798395835}{556}&\frac{16328931207}{3058}&\frac{15735207287}{12232}&\frac{2258693435}{12232}&\frac{8782801}{556}&\frac{103675}{139}&15\\-\frac{80949464718}{1529}&-\frac{338705850511}{6116}&-\frac{150907466733}{6116}&-\frac{74228837833}{12232}&-\frac{10882115811}{12232}&-\frac{43223443}{556}&-\frac{521157}{139}&-77\\\frac{347623458975}{3058}&\frac{32991350565}{278}&\frac{322759355227}{6116}&\frac{158457515673}{12232}&\frac{23184921987}{12232}&\frac{91902509}{556}&\frac{1105723}{139}&163\\-\frac{368052969807}{3058}&-\frac{190572156372}{1529}&-\frac{168114763631}{3058}&-\frac{163720428321}{12232}&-\frac{23758375953}{12232}&-\frac{93404429}{556}&-\frac{1114663}{139}&-163\\\frac{177327816597}{3058}&\frac{366011927673}{6116}&\frac{40230202855}{1529}&\frac{78121412337}{12232}&\frac{11304865929}{12232}&\frac{44328883}{556}&\frac{527737}{139}&77\\-\frac{29809040325}{3058}&-\frac{62775138251}{6116}&-\frac{28175845633}{6116}&-\frac{13970430847}{12232}&-\frac{2065443305}{12232}&-\frac{8275441}{556}&-\frac{100655}{139}&-15\\\frac{818331696}{1529}&\frac{880217988}{1529}&\frac{1617383067}{6116}&\frac{822460415}{12232}&\frac{124982969}{12232}&\frac{515919}{556}&\frac{6481}{139}&1\end{bmatrix}.\tag{4.7}$$

Moreover, these are the only P-recurrences with the corresponding order (r) and degree (d) for the three sequences. (E.g., (4.5) is the only P-recurrence with $(r,d)=(3,4)$ satisfied by the sequence (a_n).)

A proof of the first part of the proposition, namely, the sequences defined by (4.2)-(4.4) satisfy the P-recurrences (4.5)-(4.7), can be established by a refinement of Zeilberger's *creative telescoping method* [27] due to Koutschan [18] (implemented in his Mathematica package `HolonomicFunctions`.) Without diving into this method, we can check the second part of the claim in an elementary fashion. Assume that we have established that (a_n) follows a P-reccurence of order $r = 3$ and degree $d = 4$, then the $(d+1)(r+1) = 20$ coefficients in the polynomials satisfy, for every index n, a homogeneous linear equation with rational coefficients determined by the terms $a_n, a_{n+1}, a_{n+2}, a_{n+3}$. Using the first $N + 4$ terms of the sequence a_n with any $N \geqslant 20$, easily computable by (4.2), we can set up a homogeneous linear system that must be satisfied by the 20 coefficients. Using a symbolic linear solver to explicitly work out of a basis of the null space of the rational $N \times 20$ coefficient matrix – and seeing that the basis consists of one vector in $\mathbb{R}^{20}$ with a certain $N \geqslant 20$ – would not only prove the claimed uniqueness (up to an arbitrary scaling factor), but also reproduce the P-recurrence in (4.5). This method is called 'guessing' in [15], as it can be used to guess (with high confidence) what the P-recurrence might be when used with a big enough N.

Using asymptotic techniques [26, 9, 14] of holonomic functions, it can also be shown that

$$d_n \sim c \cdot \left(\sqrt{2}+1\right)^{2n} n^3 \ln(n), \quad c \approx 8.071956.... \tag{4.8}$$

This is more than enough for showing that d_n is eventually positive, but is insufficient for verifying full positivity.

5 Final Remarks

This paper connects a special case of the theory of Willmore surfaces to the theory of special functions, with the hope that it may mobilize some interests in (i) the more ambitious uniqueness question discussed in Section 1 and (ii) the positivity problem of P-recurrence, which is already a well-known open problem in combinatorics [16, 22]. With all likelihood, our approach for case (iii) of Conjecture 1.1, being specific to the Clifford torus, would not contribute much to the uniqueness problem in the other two cases Conjecture 1.1. However, it remains to see if the special function approach applies to the understanding of the higher genus Lawson surface $\xi_{g,1}$, which is conjectured to be the genus g Willmore minimizer. (Recall that the Clifford torus corresponds to $\xi_{1,1}$.)

On the other end, the ongoing work on attacking the positivity of the P-recurrence (4.7) should contribute to the general positivity problem. A key difficulty of proving positivity is that the characteristic polynomial of (4.7), namely, $z^7 - 15z^6 + 77z^5 - 163z^4 + 163z^3 - 77z^2 + 15z - 1$ has roots

$$\rho, \rho, 1, 1, 1, \rho^{-1}, \rho^{-1}, \quad \rho = \left(\sqrt{2}+1\right)^2.$$

The repeated dominant root makes a certain dynamical system associated to the recurrence unstable, which is related to why positivity is difficult to check. In contrast, the characteristic polynomials of (4.5) and (4.6), both being $z^3 - 7z^2 + 7z - 1$, have roots $\rho, 1, \rho^{-1}$; their positivity is easy to check by a simple inductive argument.

References

[1] D. E. Blair. *Inversion theory and conformal mapping.* Student mathematical library. Providence, R.I. American Mathematical Society, 2000.

[2] W. Blaschke. *Vorlesungen ber Differentialgeometrie III.* Springer, 1929.

[3] W. Boehm. On cyclides in geometric modeling. *Computer Aided Geometric Design*, 7(14):243 – 255, 1990.

[4] P. B. Canham. The minimum energy of bending as a possible explanation of the biconcave shape of the human red blood cell. *Journal of Theoretical Biology*, 26(1):61–76, 1970.

[5] V. Chandru, D. Dutta, and C. M. Hoffmann. On the geometry of Dupin cyclides. *The Visual Computer*, 5(5):277–290, 1989.

[6] B. Y. Chen. An invariant of conformal mappings. *Proc. Amer. Math. Soc.*, 40:563–564, 1973.

[7] J. Chen, T. P.-Y. Yu, P. Brogan, R. Kusner, Y. Yang, and A. Zigerelli. Numerical methods for biomembranes: conforming subdivision versus non-conforming PL methods. Submitted to Mathematics of Computation, September 2018.

[8] E. A. Evans. Bending resistance and chemically induced moments in membrane bilayers. *Biophysical Journal*, 14(12):923 – 931, 1974.

[9] P. Flajolet and R. Sedgewick. *Analytic Combinatorics*. Cambridge University Press, New York, NY, USA, 2009.

[10] W. Helfrich. Elastic properties of lipid bilayers: Theory and possible experiments. *Z. Naturforsch C*, 28(11):693–703, 1973.

[11] U. Hertrich-Jeromin. *Introduction to Möbius differential geometry*. London Mathematical Society lecture note volume 300. Cambridge University Press, 2003.

[12] G. R. Jensen, E. Musso, and L. Nicolodi. *Surfaces in Classical Geometries: A Treatment by Moving Frames*. Universitext. Springer, 1 edition, 2016.

[13] F. Jülicher, U. Seifert, and R. Lipowsky. Conformal degeneracy and conformal diffusion of vesicles. *Physical review letters*, 71(3):452–455, 1993.

[14] M. Kauers. A mathematica package for computing asymptotic expansions of solutions of P-finite recurrence equations. Technical report, RISC-Linz, 2011. Tech. Rep. 11-04.

[15] M. Kauers and P. Paule. *The Concrete Tetrahedron: Symbolic Sums, Recurrence Equations, Generating Functions, Asymptotic Estimates*. Texts and Monographs in Symbolic Computation. Springer-Verlag Wien, 1 edition, 2011.

[16] M. Kauers and V. Pillwein. When can we detect that a p-finite sequence is positive? In *Proceedings of the 2010 International Symposium on Symbolic and Algebraic Computation - ISSAC*. ACM Press, 2010.

[17] L. G. A. Keller, A. Mondino, and T. Rivière. Embedded surfaces of arbitrary genus minimizing the willmore energy under isoperimetric constraint. *Archive for Rational Mechanics and Analysis*, 212(2):645–682, May 2014.

[18] C. Koutschan. A fast approach to creative telescoping. *Mathematics in Computer Science*, 4:259–266, 2010.

[19] H. B. Lawson, Jr. Complete minimal surfaces in S^3. *Ann. of Math. (2)*, 92:335–374, 1970.

[20] J. C. Maxwell. On the cyclide. *Quarterly Journal of Pure and Applied Mathematics*, (9):111–126, 1868.

[21] X. Michalet and D. Bensimon. Observation of stable shapes and conformal diffusion in genus 2 vesicles. *Science*, 269(5224):666–8, 1995.

[22] J. Ouaknine and J. Worrell. Positivity problems for low-order linear recurrence sequences. In *Proceedings of the Twenty-Fifth Annual ACM-SIAM Symposium on Discrete Algorithms*. Society for Industrial and Applied Mathematics, dec 2013.

[23] J. Schygulla. Willmore minimizers with prescribed isoperimetric ratio. *Archive for Rational Mechanics and Analysis*, 203(3):901–941, 2012.

[24] U. Seifert. Configurations of fluid membranes and vesicles. *Advances in Physics*, 46(1):13–137, 1997.

[25] R. P. Stanley. *Enumerative combinatorics. Vol. 2*, volume 62 of *Cambridge Studies in Advanced Mathematics*. Cambridge University Press, Cambridge, 1999. With a foreword by Gian-Carlo Rota and appendix 1 by Sergey Fomin.

[26] J. Wimp and D. Zeilberger. Resurrecting the asymptotics of linear recurrences. *Journal of Mathematical Analysis and Applications*, 111:162–176, 1985.

[27] D. Zeilberger. A holonomic systems approach to special functions identities. *Journal of Computational and Applied Mathematics*, 32(3):321 – 368, 1990.